CROSSING-POINT ESTIMATION FOR SAMPLED RANDOM SIGNALS

Graeme Smecher and Benoît Champagne

Department of Electrical and Computer Engineering, McGill University
Email: graeme.smecher@mail.mcgill.ca, champagne@ece.mcgill.ca

ABSTRACT

We consider the problem of estimating the crossing points of a known carrier signal with a Gaussian random process, given uniformly-spaced, noisy samples of the random process. We derive the maximum a-posteriori (MAP) estimator for the problem, along with the Cramér-Rao bound (CRB) on estimator variance. We also derive an alternate, computationally efficient estimator using a minimum mean-squared error (MMSE) approach, and show that this MMSE estimator approximates the MAP estimator in the high-SNR regime. Simulations show that both MMSE and MAP estimators approach the CRB and outperform alternative estimators based on inverse linear and Lagrange interpolating polynomials.

***Index Terms*—** MAP Estimation, Least-Mean-Square Methods, Level-Crossing Problems, Pulse-Width Modulation

1. INTRODUCTION

The problem of accurately estimating the crossing points of an unknown signal with a known carrier occurs in several contexts, including the natural-sampling problem in Pulse-Width Modulation (PWM) [1, 2] and zero-crossing FM demodulation [3]. Often, particularly in discrete-time implementations of the above applications, only noisy uniformly-spaced samples of the random signal are available, along with a statistical characterization.

Several practical solutions to this problem may be found in the literature, ranging in complexity from straight-line interpolation between samples, to higher-order interpolators using Lagrange polynomials [1]. A summary of methods used in practice may be found in [2, 4]. These approaches do not take advantage of any statistical knowledge of the underlying signals. While these methods perform well in an oversampled regime when the random signal is low-pass in nature, they do not generalize to arbitrary signal models, and may not be as computationally efficient as alternative methods.

This paper approaches the discrete-time crossing-point estimation problem from a statistical perspective under the maximum a-posteriori (MAP) framework. Using this approach, we derive the MAP estimator and the Cramér-Rao bound (CRB) on estimator variance for the problem. We introduce an alternative estimator using the minimum mean-squared error (MMSE) estimator for the random signal, and show it to be an approximation to the MAP estimator under high-SNR conditions. We present simulated results using the sinusoid-crossing problem in click modulation [5] as a scenario. We simulate both the MAP and MMSE estimators, and compare their performance with both the Cramér-Rao bound (CRB) and the existing approaches mentioned above. The MAP and MMSE estimators approach the CRB and outperform the alternative estimators we consider.

978-1-4244-1643-1/08/$25 © 2008 IEEE

2. PROBLEM FORMULATION

We first present the discrete-time crossing-point estimation problem in its general form. We then describe a simplified approach commonly used in practice.

2.1. Discrete-Time Crossing-Point Estimation Problem

Let $s(t)$ be a continuous, real-valued, wide-sense stationary (WSS) Gaussian random process with zero mean, autocorrelation function $r_s(t-u) = E\{s(t)s(u)\}$, and variance $\sigma_s^2 = r_s(0)$. Let $y(t)$ be a known, deterministic signal. We wish to determine the crossing-points of $s(t)$ and $y(t)$, or equivalently, the zero-crossings of $z(t)$ defined as follows:

$$z(t) = s(t) - y(t). \tag{1}$$

In order to estimate these points, we are provided with a set of K consecutive uniformly-spaced noisy samples from $s(t)$. We define these noisy samples as $x[k]$, i.e.

$$x[k] = s(kT_s + T_d) + n[k] \qquad k \in \{0, 1, \ldots, K-1\} \tag{2}$$

where T_s denotes the sampling period, T_d is a known sampling offset, and $n[k]$ is an additive measurement noise. We model $n[k]$ as a WSS discrete-time Gaussian random process with zero mean and autocorrelation $r_n[k-l] = \sigma_n^2\delta[k-l]$, where σ_n^2 denotes the variance and δ is the Kronecker delta function.

The discrete-time crossing-point estimation problem may be stated as follows. Given $y(t)$ and K samples $x[k]$, estimate the points $\tau_0 < \tau_1 < \cdots$ satisfying $s(\tau_i) = y(\tau_i)$, or equivalently, $z(\tau_i) = 0$.

Because K is arbitrary and the number of crossings is not limited, the complexity of this problem is unbounded. In the following section, we describe a two-step approach which simplifies the discrete-time crossing-point estimation problem.

2.2. Simplified Discrete-Time Crossing-Point Estimation

Following published approaches to the discrete-time crossing-point estimation problem [1, 2, 4] we impose a two-step structure on our solution to the general problem. We first define $\xi[k]$ as follows:

$$\xi[k] = x[k] - y(kT_s + T_d) \tag{3}$$

In the first step, $\xi[k]$ is monitored for changes in sign. When the noise term is sufficiently small, $\xi[k] \approx z(kT_s + T_d)$. Thus, neglecting the possibility that multiple zero crossings occur within each sampling interval, sign changes in $\xi[k]$ coarsely bound each zero crossing τ_i to a single sample interval. When $\xi[k-1]\xi[k] < 0$, we have:

$$\tau_i \in \mathcal{T}_i \triangleq ([k-1]T_s + T_d, kT_s + T_d) \tag{4}$$

The vanishing probability that the zero crossing occurs precisely on a sampling instant is neglected.

The second step of the simplified discrete-time crossing-point estimation problem is defined as follows. Let the vector $\mathbf{x}$ denote $M = M_1 + M_2$ consecutive samples from $x[k]$ surrounding a single crossing point τ_i:

$$\mathbf{x} = [\, x[k-M_1], \ldots, x[k-1], x[k], \ldots, x[k+M_2-1] \,]^T \quad (5)$$

Given $y(t)$, the sample vector $\mathbf{x}$, and the bracketing interval (4) for the ith zero crossing of $z(t)$, find an estimate $\hat{\tau}_i$ of the true crossing time τ_i.

In the sequel, we focus on the second step of the simplified problem in order to exploit statistical knowledge of $\mathbf{x}$.

3. DERIVATION OF MAP AND MMSE ESTIMATORS

Let $f(\tau|\mathbf{x})$ be the probability density function (pdf) of a zero crossing of $z(t)$ at time $t = \tau \in \mathcal{T}$ conditioned on the sample vector $\mathbf{x}$. The MAP estimate of τ maximizes this function, i.e.:

$$\hat{\tau}_{\text{MAP}} = \underset{\tau}{\operatorname{argmax}}\, f(\tau|\mathbf{x})$$

Let $f(\tau)$ represent the pdf of a zero crossing at time τ. Further, let $f(\mathbf{x}|\tau)$ be the conditional probability density function of sample vector $\mathbf{x}$ given a zero crossing at τ. The MAP estimate $\hat{\tau}_{\text{MAP}}$ satisfies the canonical MAP equation: [6]

$$\left.\frac{d}{d\tau}\log f(\mathbf{x}|\tau)\right|_{\tau=\hat{\tau}_{\text{MAP}}} = -\left.\frac{d}{d\tau}\log f(\tau)\right|_{\tau=\hat{\tau}_{\text{MAP}}}$$

We define $S(\mathbf{x}|\tau)$ as follows:

$$S(\mathbf{x}|\tau) \triangleq \frac{d}{d\tau}\log f(\mathbf{x}|\tau) \quad (6)$$

We also assume an uniform (uninformative) a-priori distribution $f(\tau)$, although generalizations are possible. (For example, the a-priori distribution $f(\tau)$ of zero crossings is well-studied [16, 17] when $y(t)$ is a sinusoid.) When $f(\tau)$ is uniform, $d\log f(\tau)/d\tau = 0$ and the MAP estimate satisfies

$$S(\mathbf{x}|\tau)|_{\tau=\hat{\tau}_{\text{MAP}}} = 0 \quad (7)$$

We express componentwise derivatives of scalars, vectors, and matrices (which are always with respect to τ) using a dot notation. For example, $\dot{y}(\tau) \triangleq dy(\tau)/d\tau$.

In order to express (7), we require the pdf $f(\mathbf{x}|\tau)$. We begin by considering the unconditional sample-vector pdf $f(\mathbf{x})$. We then condition on τ, giving $f(\mathbf{x}|\tau)$. Expressions for these distributions are derived in the next section.

3.1. Sample Vector Distribution

Consider the discrete-time random process $x[k]$ given by (2). Because $s(t)$ and $n[k]$ are statistically independent, jointly Gaussian processes, $x[k]$ is Gaussian with zero mean, variance $\sigma^2 = \sigma_s^2 + \sigma_n^2$, and autocorrelation $r[k] = r_s(kT_s) + \sigma_n^2\delta[k]$. The pdf $f(\mathbf{x})$ takes the standard Gaussian form:

$$f(\mathbf{x}) = \frac{1}{(2\pi)^{M/2}|\Sigma_0|^{1/2}}\exp\left(-\frac{1}{2}\mathbf{x}^T\Sigma_0^{-1}\mathbf{x}\right)$$

where Σ_0 is an $M \times M$ symmetric Toeplitz covariance matrix. We introduce the correlation vector function $\boldsymbol{\rho}(t)$ defined as follows:

$$\boldsymbol{\rho}(t) = \begin{bmatrix} r_s\left(t - [k-M_1]T_s - T_d\right) \\ \vdots \\ r_s\left(t - [k+M_2-1]T_s - T_d\right) \end{bmatrix}.$$

Now, Σ_0 may be expressed in terms of $\rho(t)$ as

$$\Sigma_0 = \begin{bmatrix} \boldsymbol{\rho}\left([k-M_1]T_s + T_d\right)^T \\ \vdots \\ \boldsymbol{\rho}\left([k+M_2-1]T_s + T_d\right)^T \end{bmatrix} + \sigma_n^2 I \quad (8)$$

where I is the $M \times M$ identity matrix.

We now consider the distribution of the vector $\mathbf{x}$ conditioned on a zero crossing of $z(t)$ at τ. From (1), $s(\tau) = y(\tau)$, and we form the augmented sample vector

$$\mathbf{x}_\tau = [\, \mathbf{x}^T \,,\; s(\tau) \,]^T = [\, (\mathbf{n}^T + \mathbf{s}^T) \,,\; s(\tau) \,]^T \quad (9)$$

where $\mathbf{n}$ and $\mathbf{s}$ denote, respectively, the components of $\mathbf{x}$ due to the noise process $n[k]$ and signal process $s(t)$. As $\mathbf{n}$ and $\mathbf{s}$ are jointly Gaussian, $\mathbf{x}_\tau$ is a Gaussian random vector with zero mean and covariance matrix Σ_τ which may be expressed in partitioned form as follows:

$$\Sigma_\tau = \left[\begin{array}{c:c} \Sigma_0 & \boldsymbol{\rho}(\tau) \\ \hdashline \boldsymbol{\rho}(\tau)^T & \sigma_s^2 \end{array}\right] \quad (10)$$

The conditional distribution of $\mathbf{x}$ given τ is equivalent to the addition of a new random variable with a known value, i.e. $s(\tau) = y(\tau)$. The pdf $f(\mathbf{x}|\tau)$ is Gaussian with conditional covariance matrix $\Sigma(\tau)$ and conditional mean $\boldsymbol{\mu}(\tau)$ defined as follows: [7]

$$\Sigma(\tau) = \Sigma_0 - \sigma_s^{-2}\boldsymbol{\rho}(\tau)\boldsymbol{\rho}^T(\tau) \quad (11)$$

$$\boldsymbol{\mu}(\tau) = \boldsymbol{\rho}(\tau)\sigma_s^{-2}y(\tau) \quad (12)$$

In the following development, we suppress dependence of y, $\boldsymbol{\rho}$, Σ and $\boldsymbol{\mu}$ on τ to simplify notation. We have:

$$f(\mathbf{x}|\tau) = \frac{\exp\left(-\frac{1}{2}(\mathbf{x}-\boldsymbol{\mu})^T\Sigma^{-1}(\mathbf{x}-\boldsymbol{\mu})\right)}{(2\pi)^{M/2}|\Sigma|^{1/2}} \quad (13)$$

These expressions completely characterize the conditional distribution $f(\mathbf{x}|\tau)$. We now continue deriving the MAP estimator.

3.2. MAP Derivation

The MAP estimate of τ satisfies (7). In order to derive the MAP estimator, we require an expression for $S(\mathbf{x}|\tau)$. Combining (13) and (6), we have:

$$S(\mathbf{x}|\tau) = -\frac{1}{2}\frac{d}{d\tau}\left[\log|\Sigma| + (\mathbf{x}-\boldsymbol{\mu})^T\Sigma^{-1}(\mathbf{x}-\boldsymbol{\mu})\right] \quad (14)$$

To simplify this expression, we introduce the following definitions:

$$\begin{aligned} a &= \boldsymbol{\rho}^T\Sigma^{-1}\boldsymbol{\rho}/\sigma_s^2 \qquad & c &= \mathbf{x}^T\Sigma^{-1}\boldsymbol{\rho} \\ b &= \boldsymbol{\rho}^T\Sigma^{-1}\dot{\boldsymbol{\rho}}/\sigma_s^2 \qquad & d &= \mathbf{x}^T\Sigma^{-1}\dot{\boldsymbol{\rho}} \end{aligned} \quad (15)$$

With some manipulations and elementary identities for differentiating matrix expressions, (14) may be expressed as follows:

$$S(\mathbf{x}|\tau) = b - \frac{(ay-c)(by-d) + \dot{y}(ay-c) + y(by-d)}{\sigma_s^2} \quad (16)$$

Due to the terms a, b, c, and d, this form for $S(\mathbf{x}|\tau)$ still depends on the conditional covariance matrix Σ, which in turn depends on τ. We may use the Sherman-Morrison-Woodbury formula [8] to express Σ^{-1} in terms of Σ_0^{-1}:

$$\Sigma^{-1} = \Sigma_0^{-1} + \frac{\Sigma_0^{-1}\boldsymbol{\rho}\boldsymbol{\rho}^T\Sigma_0^{-1}}{\sigma_s^2 - \boldsymbol{\rho}^T\Sigma_0^{-1}\boldsymbol{\rho}} \tag{17}$$

This formula is valid provided that Σ_0 is nonsingular (which may be guaranteed by construction) and provided $\sigma_s^2 \neq \boldsymbol{\rho}^T\Sigma_0^{-1}\boldsymbol{\rho}$, which is guaranteed if $\sigma_n^2 \neq 0$. Let:

$$\begin{aligned} a_0 &= \boldsymbol{\rho}^T\Sigma_0^{-1}\boldsymbol{\rho}/\sigma_s^2 \qquad & c_0 &= \mathbf{x}^T\Sigma_0^{-1}\boldsymbol{\rho} \\ b_0 &= \boldsymbol{\rho}^T\Sigma_0^{-1}\dot{\boldsymbol{\rho}}/\sigma_s^2 \qquad & d_0 &= \mathbf{x}^T\Sigma_0^{-1}\dot{\boldsymbol{\rho}} \end{aligned} \tag{18}$$

We apply (17) to each of the equations (15) and express the result using (18). Using these identities, (16) may be expressed as:

$$\begin{aligned} S(\mathbf{x}|\tau) = \frac{d_0 y}{\sigma_s^2} &- \frac{b_0(a_0 y - c_0)(y - c_0)}{\sigma_s^2(1-a_0)^2} \\ &+ \frac{b_0\sigma_s^2 + (d_0 - \dot{y})(a_0 y - c_0) - y b_0(y - c_0)}{\sigma_s^2(1-a_0)} \end{aligned} \tag{19}$$

The MAP estimate $\hat{\tau}_{\mathrm{MAP}}$ corresponds to roots of (19). In practice, zero-finding method such as Brent's algorithm [9] or Newton's method may be applied.

Naïvely applied root-finding methods are both numerically sensitive and computationally expensive. To design a more efficient estimator, we will make a number of approximations in order to simplify (19). In doing so, we will arrive at a MMSE formulation for the problem.

3.3. MMSE Derivation

Consider the minimum mean-squared error (MMSE) estimate $\hat{s}(\tau)$ of $s(\tau)$ at arbitrary τ given the vector $\mathbf{x}$ of nearby samples. This estimate is given by the Wiener-Hopf equation: [10]

$$\hat{s}(\tau) = \boldsymbol{\rho}(\tau)^T\Sigma_0^{-1}\mathbf{x} = c_0$$

The expected mean-squared error for this estimate is given by: [10]

$$\epsilon = \sigma_s^2 - \boldsymbol{\rho}(\tau)^T\Sigma_0^{-1}\boldsymbol{\rho}(\tau) = \sigma_s^2(1-a_0)$$

As ϵ is a variance and Σ_0 is nonnegative definite, $\epsilon \in [0, \sigma_s^2]$. We may consider ϵ to be a measure of confidence in $\hat{s}(\tau)$. When $\mathbf{x}$ consists of samples near τ, and assuming a modest oversampling rate, we should expect this error to be small compared to σ_s^2.

Due to the 2-step structure of our estimator, $\tau \in \mathcal{T}$. This bound allows us to choose a vector $\mathbf{x}$ of nearby samples such that $1 - a_0$ is small over the region of possible zero crossings. When this is the case, the second term on the right-hand side of (19) dominates. We define the MMSE estimate $\hat{\tau}_{\mathrm{MMSE}}$, which satisfies:

$$\begin{aligned} S(\mathbf{x}|\tau)\big|_{\tau=\hat{\tau}_{\mathrm{MMSE}}} &\approx \left.\frac{b_0(a_0 y - c_0)(y - c_0)}{(1-a_0)^2}\right|_{\tau=\hat{\tau}_{\mathrm{MMSE}}} \\ &\approx \left.\frac{b_0(y-c_0)^2}{(1-a_0)^2}\right|_{\tau=\hat{\tau}_{\mathrm{MMSE}}} \approx 0 \end{aligned} \tag{20}$$

The approximated MAP estimate corresponds to solutions of this equation. The two candidates are roots of b_0 and $y - c_0$. However, as b_0 is a function of τ and Σ_0^{-1} only, it does not involve the sample vector in any way. This term may contribute only static solutions to the estimator equation, which we may disregard.

Thus, the MMSE estimate satisfies:

$$\hat{\tau}_{\mathrm{MMSE}} = \arg_\tau \left[\mathbf{x}^T\Sigma_0^{-1}\boldsymbol{\rho}(\tau) = y(\tau)\right] \tag{21}$$

This result relates the MMSE estimate of $s(\tau)$ to the carrier signal. It is comparable to the Wiener-Hopf equations, except that in contrast to the usual situation, τ is unknown and $y(\tau)$ is known.

A more intuitive interpretation follows. The expression $\mathbf{x}^T\Sigma_0^{-1}\boldsymbol{\rho}$ defines a family of interpolating estimators for the unknown signal $s(\tau)$. When parameterized by the sample vector $\mathbf{x}$, this estimator is a function only of the time variable τ. We seek τ such that this function equals the carrier function $y(\tau)$.

Since both the carrier signal and $\boldsymbol{\rho}(\tau)$ are in general nonlinear functions, a line-search method must once again be adopted.

3.4. Fundamental Performance Limits

The Cramér-Rao bound for the random parameter τ bounds the variance $\sigma_{\hat{\tau}}^2$ of any unbiased estimator as follows: [6]

$$\sigma_{\hat{\tau}}^2 \geq \left[E_\tau\left\{\mathcal{I}_\tau\right\}\right]^{-1} \tag{22}$$

where $E_\tau\{\,\cdot\,\}$ denotes the statistical expectation operator with respect to τ, and $\mathcal{I}_\tau$ is the Fisher information for the random parameter τ given as follows: [11]

$$\mathcal{I}_\tau = \dot{\boldsymbol{\mu}}^T\Sigma^{-1}\dot{\boldsymbol{\mu}} + \frac{1}{2}\,\mathrm{tr}\left[\Sigma^{-1}\dot{\Sigma}\Sigma^{-1}\dot{\Sigma}\right] \tag{23}$$

This expression may readily be simplified using the notation introduced in (15). With the additional definition $e = \dot{\boldsymbol{\rho}}^T\Sigma^{-1}\dot{\boldsymbol{\rho}}/\sigma_s^2$, the result is as follows:

$$\mathcal{I}_\tau = \frac{ey^2 + 2by\dot{y} + a\dot{y}^2}{\sigma_s^2} + b^2 + ae$$

As before, it is desirable to express $\mathcal{I}_\tau$ without using the conditional covariance matrix Σ. Accordingly, we define $e_0 = \dot{\boldsymbol{\rho}}^T\Sigma_0^{-1}\dot{\boldsymbol{\rho}}/\sigma_s^2$ and use the expressions (17) and (18):

$$\begin{aligned} \mathcal{I}_\tau = &\frac{b_0^2 y^2 + 2b_0 y\dot{y} + a_0\dot{y}^2}{\sigma_s^2(1-a_0)} + \frac{a_0 e_0}{1-a_0} \\ &+ \frac{b_0^2(1+a_0)}{(1-a_0)^2} + \frac{e_0 y^2}{\sigma_s^2} \end{aligned} \tag{24}$$

This expression is averaged over values of τ by the expectation operator in (22). How this expectation is evaluated depends on the form of $y(t)$ and hence the application. In a normally operating click- or pulse-width modulation system, $y(t)$ is periodic and the crossing points we wish to estimate are a-priori guaranteed to occur exactly once per half-period (or full period, in the case of sawtooth PWM.) In these applications, it is possible to determine the Cramér-Rao bound by taking the expectation in (22) over a single half- or full-period of $y(t)$.

4. PERFORMANCE SIMULATION

In the following subsections, we introduce a test scenario, describe the signal models used, and briefly review a number of alternative estimators used to evaluate the performance of our approach. We then present some simulation results.

4.1. Scenario and Methodology

We assume a strictly bandlimited model for $s(t)$; thus, $r_s(t) = \sigma_s^2 \operatorname{sinc}(\omega t/\pi)$. We also adopt a sinusoidal carrier $y(t) = A\cos(\omega t + \theta)$ in order to derive an estimator useful for click modulation [5]. Note that the carrier frequency ω and the bandlimit of $s(t)$ are identical in this scenario.

In addition to regular samples from $s(t)$, we require precise knowledge of each crossing point in order to determine the error for each estimator. To do this, it is useful to generate $s(t)$ in such a way that it may be evaluated at arbitrary time instants. We begin with the Karhunen-Loève expansion for the bandlimited signal $s(t)$:

$$s(t) = \underset{N\to\infty}{\mathrm{l.i.m.}} \sum_{n=1}^{N} s_n \psi_n(t) \quad t_0 \le t \le t_{M-1} \tag{25}$$

where $\mathrm{l.i.m.}$ represents the limit in the mean-squared sense. For strictly bandlimited spectra, the functions $\psi_n(t)$ are scaled Prolate Spheroidal Wave Functions (PSWFs) [6, 12, 13]. The corresponding s_n are uncorrelated, zero-mean Gaussian random variables with variance λ_n, where λ_n are parameter-dependent eigenvalues associated with each eigenfunction $\psi_n(t)$. We generate the PSWFs and associated eigenvalues according to the procedures outlined in [14, 15].

In practice, the expected energy λ_n associated with each eigenfunction within the observation interval decreases rapidly as n increases, and the summation in (25) may be truncated. We truncate the summation when additional terms contribute less than 10^{-10} of the total energy in $s(t)$ over the observation interval. Depending on the scenario being simulated, this requires between 6 and 10 terms.

For each simulation, segments of $s(t)$ of length $(M-1)T_s$ are generated randomly. The carrier phase θ of $y(t)$ is chosen randomly, and $z(t) = s(t) - y(t)$ is formed. We then sample and add noise, forming the observation vector $\mathbf{x}$. This sample vector (and the underlying $z(t)$) are not a-priori guaranteed to have a zero-crossing in $\mathcal{T}$; candidates that do not have a zero crossing in the desired region are discarded.

4.2. Reference Estimators

In addition to the MAP and MMSE estimators corresponding to (19) and (21), and the Cramér-Rao bound given in (22) and (24), we evaluate a number of alternative estimators. These estimators are taken from the literature and are useful for comparison.

The following list introduces acronyms used to identify both the reference estimators and the quantities derived above.

CRB Cramér-Rao Bound.

UB Upper-bound estimator; selects randomly from an uniform distribution on $\mathcal{T}$. Variance is $T_s^2/12$.

MAP Exact MAP estimator; solves for nearby root of (19).

MMSE Approximation to MAP estimator given by (21).

POL Solution to $\hat{\xi}(t) = 0$, where $\hat{\xi}(t)$ is the unique Lagrange interpolating polynomial of degree $M-1$ satisfying $\xi[n] = \hat{\xi}(nT_s + T_d)$ at the M samples of $\mathbf{x}$. See e.g. [2].

ILIN Linear interpolation between the nearest samples of $\xi[k]$ defined in (3). This method may be viewed as a degenerate case of the POL method. See e.g. [2].

Parameter	Value	Description
T_s^{-1}	192 kHz	sampling rate
$\omega/2\pi$	24 kHz	bandlimit of $s(t)$
M	4	number of samples
A	1	carrier amplitude
σ_n^2	$\left(2^{-15}\right)^2/12$	noise variance
σ_s^2	$(1/4)^2$	signal variance

Table 1. Operating point parameters

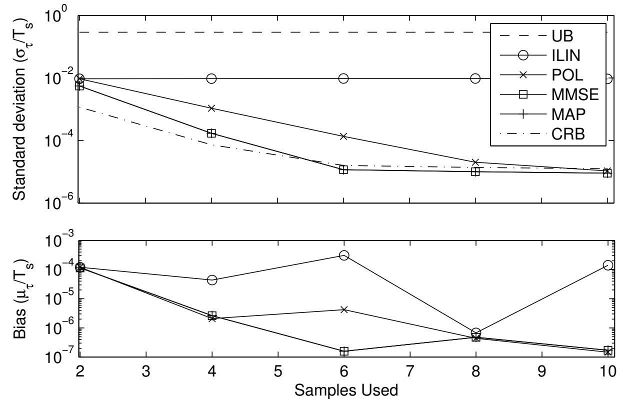

Fig. 1. Estimator performance; number of samples M varies

4.3. Results

Each of the following plots is generated by varying a single parameter, where the others are held at the operating point described in Table 1. Each data point in the following plots corresponds to the results from approximately 3000 simulations.

For each data point, outliers corresponding to crossing-point estimates outside (4) have been removed. Outliers of this type are readily identifiable in a practical estimator. In the simulations reviewed here, outliers are only generated at the low-SNR range in Figure 3. The frequencies of these outliers are described below.

The noise variance has been chosen to model 16-bit quantization noise, which represents a minimal amount of distortion in high-quality audio recordings. The signal variance has been chosen to provide a reasonable dynamic range with minimal probability that the input signal has an amplitude greater than the carrier (an undesirable condition known as modulator overload.) The sampling rate and bandlimit of $s(t)$ are design details, for which we have attempted to choose reasonable values.

Figure 1 shows the estimator performance as the number of samples is varied over the even numbers between 2 and 10. The CRB, POL, MMSE, and MAP estimators rapidly approach a limit beyond which more samples do not improve performance. The ILIN estimator, in all cases, only uses 2 samples.

Figure 2 shows the estimator performance as a function of the oversampling rate. The horizontal axis is normalized to the sampling rate so that 1 corresponds to Nyquist-rate sampling. Data near critical (Nyquist-rate) sampling has been omitted because in this region, the assumptions of our two-step estimator (i.e. the that zero crossings are well-separated when $s(t)$ is sampled) are not satisfied.

Figure 3 shows the estimator performance as the SNR (σ_s/σ_n, shown in dB) is varied. For high-fidelity switching amplifiers, the SNR may be well over 90 dB. In the high-SNR regime, when high accuracy is required, the MAP and MMSE estimators have an ad-

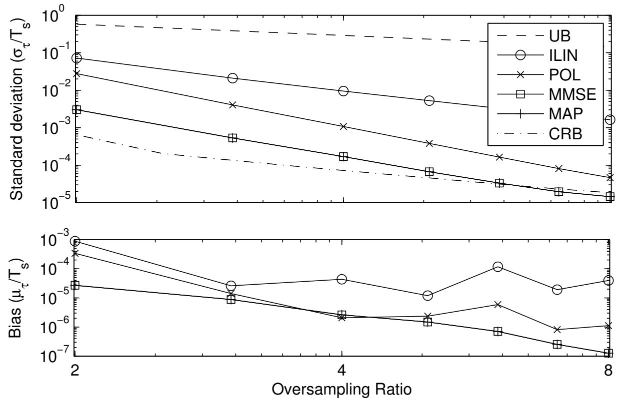

Fig. 2. Estimator performance; oversampling ratio varies

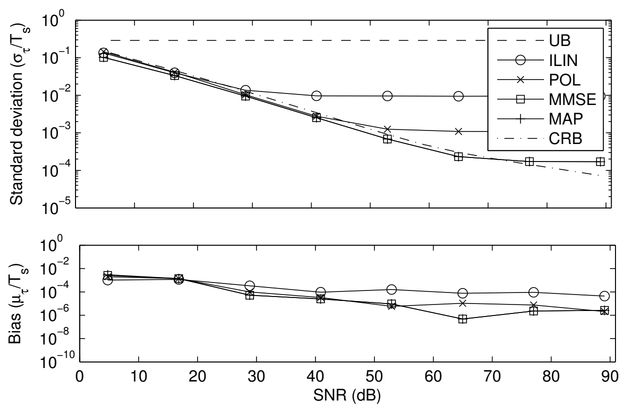

Fig. 3. Estimator performance; SNR varies

vantage over the POL and ILIN estimators. In this scenario, outliers were generated at the lowest three SNRs for the MAP (4%, 1%, and 0.2%) and MMSE (4%, 1%, and 0.2%) estimators.

In certain cases, the estimator surpasses the calculated Cramér-Rao bound. This is due to our assumption that $f(\tau)$ is uniformly distributed in (24). Because $s(t)$ is zero-mean, crossing points are a-priori most likely to occur in the neighbourhood of $y(t) = 0$. However, when $y(t)$ is sinusoidal, the carrier slew $\dot{y}(t)$ is also maximized when $y(t) = 0$. This combination produces the most accurate crossing-point estimates precisely where they are most likely to occur. Preliminary results show the Cramér-Rao bound to be below each estimator's performance when $f(\tau)$ is correctly modeled.

5. DISCUSSION

Lagrange interpolation performs well when the underlying signal $s(t)$ is low-pass and sufficiently oversampled. Unlike the methods we introduce, the Lagrange method does not generalize to arbitrary signal and noise models.

In real-time applications such as switching amplifiers, the viability of an algorithm depends on its computational cost. Accordingly, the POL and MMSE estimators are the chief competitors among the estimators we have examined. Both Lagrange interpolation [18] and the MMSE estimator (21) may be posed as a zero-finding problem using a convolutional filter with time-varying taps to interpolate the random signal $s(t)$. Thus, in terms of computational cost, the chief difference between POL and MMSE is how the taps are computed. Exploration of this process is to be evaluated in a later work.

6. REFERENCES

[1] K. Nguyen and D. Sarwate, "Up-sampling and natural sample value computation for digital pulse width modulators," in *Proc. 40th Ann. Conf. on Info. Sci. and Syst.*, March 2006, pp. 1096–1101.

[2] C. Pascual and P. D. Krein, "High-fidelity PWM inverter for digital audio amplification based on real-time DSP," *IEEE Trans. Power Electron.*, vol. 18, no. 1, pp. 473–485, 2003.

[3] T. Scholand, A. Burnic, C. Spiegel, A. Waadt, A. Hessamian-Alinejad, and P. Jung, "Applying zero-crossing demodulation to the Bluetooth enhanced data rate mode," in *Proc. IEEE Personal, Indoor and Mobile Radio Comm.*, September 2006, pp. 1–5.

[4] B.-H. Gwee, J. S. Chang, and V. Adrian, "A micropower low-distortion digital class-D amplifier based on an algorithmic pulsewidth modulator," *IEEE Trans. Circuits Syst. I*, vol. 52, no. 10, pp. 2007–2022, 2005.

[5] B. F. Logan, "Click modulation," *AT&T Bell Labs Tech. J.*, vol. 63, no. 3, pp. 401, 1984.

[6] H. L. Van Trees, *Detection, Estimation, and Modulation Theory*, John Wiley and Sons, Inc., 1968.

[7] A. C. Rencher, *Multivariate Statistical Inference and Applications*, John Wiley & Sons, 1998.

[8] G. Golub and C. Van Loan, *Matrix Computations*, Johns Hopkins University Press, 1996.

[9] W. H. Press, *Numerical Recipes in C*, Cambridge University Press, 1988.

[10] S. Haykin, *Adaptive Filter Theory*, Prentice Hall, 1991.

[11] B. Porat and B. Friedlander, "Computation of the exact information matrix of Gaussian time series with stationary random components," *IEEE Trans. Acoustics, Speech, and Signal Processing*, vol. ASSP-34, no. 1, pp. 118–130, 1986.

[12] D. Slepian and H. O. Pollak, "Prolate spheroidal wave functions, Fourier analysis and uncertainty – I," *Bell Sys. Tech. J.*, vol. 40, pp. 43–63, 1961.

[13] H. J. Landau and H. O. Pollak, "Prolate spheroidal wave functions, Fourier analysis and uncertainty – II," *Bell Sys. Tech. J.*, vol. 40, pp. 65–84, 1961.

[14] H. Xiao, V. Rokhlin, and N. Yarvin, "Prolate spheroidal wavefunctions, quadrature and interpolation," *Inverse Problems*, vol. 17, pp. 805–838, 2001.

[15] J. P. Boyd, "Algorithm 840: Computation of grid points, quadrature weights and derivatives for spectral element methods using prolate spheroidal wave functions–prolate elements," *AC Trans. Math. Software*, vol. 31, no. 1, pp. 149–165, 2005.

[16] S. O. Rice, "Mathematical Analysis of Random Noise," in *Selected Papers on Noise and Stochastic Processes*, Nelson Wax, Ed., pp. 133–294. Dover Publications, 1954, reprinted from Bell Sys. Tech. J., vols. 23 & 24.

[17] S. Cobb, "The distribution of intervals between zero crossings of sine wave plus random noise and allied topics," *IEEE Trans. Inf. Theory*, vol. 11, no. 2, pp. 220–233, 1965.

[18] T. I. Laakso, V. Valimaki, M. Karjalainen, and U. K. Laine, "Splitting the unit delay," *IEEE Signal Process. Mag.*, vol. 13, no. 1, pp. 30–60, 1996.

Intentional Blank Page